The Journal of Experimental Biology 201, 2061–2070 (1998)
Printed in Great Britain © The Company of Biologists Limited 1998
JEB1405

DIVING SPEEDS AND ANGLES OF A GYRFALCON (*FALCO RUSTICOLUS*)

VANCE A. TUCKER[1,*], TOM J. CADE[2] AND ALICE E. TUCKER[1]

[1]*Department of Zoology, Duke University, Durham, NC 27708, USA* and [2]*The Peregrine Fund, Inc., 566 Flying Hawk Lane, Boise, ID 83709, USA*

*e-mail: vtucker@acpub.duke.edu

Accepted 23 April; published on WWW 11 June 1998

Summary

An optical tracking device recorded the three-dimensional paths of 11 dives by a 1.02 kg gyrfalcon, trained to dive to a falconer. The dives started at altitudes up to 500 m above the ground and were inclined at angles of 17–62 ° from the horizontal. The falcon controlled its speed during the dives, rather than simply falling from the sky, and the dives had three phases. During the first (acceleration) phase, the falcon accelerated to speed limits between 52 and 58 m s^{-1} in the seven fastest dives, evidently with minimum drag, because its accelerations were close to those predicted from theory for minimum drag. The falcon then began a constant-speed phase by increasing drag by a factor of 1.3–4.8 while still 100–350 m above the ground in most dives. The constant-speed phase lasted no more than a few seconds, and the falcon then began a deceleration phase by increasing its drag further, this time by factors of 1.7–3.2, and decelerating with a mean value of –0.95 times gravitational acceleration.

During all three phases, the dive angle was nearly constant or increased during the deceleration phase, and the falcon made no changes in its body shape that were obvious through the tracking device telescope except to reduce its wing span as it accelerated. The falconer, however, was close to the falcon at the end of the dive and could see that, during the deceleration phase, the falcon held its wings in a cupped position, apparently with a high angle of attack and therefore high drag. At the end of the deceleration phase, the falcon dropped its legs, spread its toes and finally spread its wings as it approached the falconer.

Although the speeds reported here are the fastest ever measured with known accuracy in animals, the falcon could theoretically have reached more than 70 m s^{-1} if it had continued to accelerate with minimum drag until close to the ground. Even at this speed, it would have had enough altitude to pull out of the dive before crashing into the ground. Several authors have estimated that diving falcons reach speeds of more than 70 m s^{-1}, and wild falcons may reach such speeds when they make long, steep dives upon birds flying high in the air.

Key words: falcon, flight, diving, gyrfalcon, *Falco rusticolus*, speed.

Introduction

Several species of falcons (genus *Falco*) feed primarily on birds, which they strike in the air after long, steep dives. A diving falcon folds its wings and appears to fall from the sky at speeds that are probably the highest reached by any animal: estimates range up to 157 m s^{-1} (Tucker, 1998). A theoretical analysis of diving, based on aerodynamic measurements on falcons flying at low speeds, shows that the speed in a dive depends on the dive angle and the duration of the dive and that speeds in excess of 100 m s^{-1} are plausible for large falcons in long, steep dives if the falcon adjusts its shape to minimize drag (Tucker, 1998). Two questions arise: does the theory describe real falcons, and do real falcons arrange themselves to have minimum drag in a dive?

The present study investigates these questions by recording the three-dimensional paths of dives performed by a gyrfalcon (*F. rusticolus*) trained to fly high above the ground and then dive to a falconer when called. Gyrfalcons are the largest of all falcons, and are thought to be the fastest fliers (Cade, 1982).

Theory

Tucker's theory (1998) describes 'ideal falcons', which are mathematical abstractions with specified aerodynamic properties and with wing spans and body dimensions that are mathematical functions of body mass between 0.5 and 2.0 kg. These properties and functions were derived from measurements on real falcons, and the diving performances of ideal and real falcons are thought to resemble one another to the extent that our knowledge of aerodynamics allows. We use some of the quantities and nomenclature from the theory (Tucker, 1998) to describe the gyrfalcon in the present study, with one addition: ideal falcons move in a vertical plane, while the gyrfalcon moved through three-dimensional space. Below,

we describe the quantities that we used to describe the gyrfalcon and the method for reducing its motion from three to two dimensions.

Coordinate system

The falcon moves relative to a three-dimensional, orthogonal, right-handed coordinate system in which the *x* and *y* axes are horizontal, and the *z* axis is vertical with its origin at the surface of the ground. The coordinate system moves with the wind without acceleration, so motions of the falcon are relative to the air and in an inertial frame of reference. The wind has vertical velocity components, but we assume that these are insignificant during a dive compared with the large vertical component of the falcon's velocity.

Glide path, dive angle and acceleration

The falcon moves along a three-dimensional glide path at speed V, which is the change in three-dimensional distance (s) along the glide path with time (t):

$$V = \mathrm{d}s/\mathrm{d}t\,. \tag{1}$$

We illustrate glide paths in two dimensions by plotting z against s_{xy}, the distance along the projection of the glide path on the x,y plane. Both z and V are functions of s_{xy}, and we show the relationship between them by plotting them both on the same graph.

The slopes of the curves for z and V determine the dive angle (Θ) and the acceleration ($\mathrm{d}V/\mathrm{d}t$), respectively. The slope $\mathrm{d}z/\mathrm{d}s_{xy}$ is the slope of the glide path, and

$$\Theta = -\tan^{-1}(\mathrm{d}z/\mathrm{d}s_{xy})\,, \tag{2}$$

where Θ is the angle of the glide path measured from the horizontal. The slope $\mathrm{d}V/\mathrm{d}s_{xy}$ is related to the acceleration ($\mathrm{d}V/\mathrm{d}t$) by the chain rule of calculus:

$$\mathrm{d}V/\mathrm{d}t = (\mathrm{d}V/\mathrm{d}s_{xy})(\mathrm{d}s_{xy}/\mathrm{d}t)\,. \tag{3}$$

Since

$$\mathrm{d}s_{xy}/\mathrm{d}t = V\cos\Theta\,, \tag{4}$$

$$\mathrm{d}V/\mathrm{d}t = (\mathrm{d}V/\mathrm{d}s_{xy})V\cos\Theta\,. \tag{5}$$

The glide paths during the dives in this study can be approximated by straight lines in space. A straight glide path has a constant dive angle, and the projected position of the bird on the x,y plane moves in a straight line.

Gravitational and aerodynamic forces on the falcon

The gravitational force on the falcon (its weight) is a constant vector that points vertically downwards. Except when Θ=0, weight has components that are parallel and perpendicular to the glide path, and the parallel component is $m\boldsymbol{g}\sin\Theta$, where m is body mass and g is the magnitude of gravitational acceleration.

The aerodynamic force (described in detail by Tucker, 1998) on the falcon is a varying vector that has two components – lift and drag – and depends on the falcon's speed and on the position of its body and wings. Lift is perpendicular to the glide path in a vertical plane and is constant as speed changes when the falcon dives at a given angle. Drag is parallel to the glide path and may vary with speed.

Acceleration

The drag (D) and gravitational force component parallel to the glide path determine the acceleration during a dive:

$$\mathrm{d}V/\mathrm{d}t = (mg\sin\Theta - D)/m\,. \tag{6}$$

We describe the falcon as accelerating, flying at constant speed or decelerating, according to whether acceleration is positive, zero or negative, respectively. At the start of a dive, $mg\sin\Theta$ is greater than drag, and the falcon accelerates. Acceleration is maximum at a given speed if the falcon adjusts the position of its wings and body to minimize drag at that speed, subject to the constraint that lift must remain constant for a given dive angle.

As the falcon accelerates, drag increases until it equals $mg\sin\Theta$, and the falcon's speed becomes constant. This situation occurs at two constant speeds that arise in this study: terminal speeds and speed limits (V_E and V_e respectively in Tucker, 1998). At terminal speeds, the falcon has arranged itself to have minimum drag and has reached the fastest speed that it can achieve at a particular dive angle; but at speed limits, the falcon has arranged itself to have more than minimum drag. Consequently, there is one terminal speed at a given glide angle, but there are an infinite number of speed limits that are always less than the terminal speed.

For example, a falcon that has stopped accelerating at a speed limit has drag equal to $mg\sin\Theta$, but it may have a wing span larger than that for minimum drag. Were it to reduce its wing span, it could decrease drag to less than $mg\sin\Theta$, and it would then accelerate until drag again equalled $mg\sin\Theta$. If its drag were then minimal, its speed would be the terminal speed.

The drag of the falcon depends on its dive angle and acceleration, as can be seen by rearranging equation 6:

$$D = m(g\sin\Theta - \mathrm{d}V/\mathrm{d}t)\,. \tag{7}$$

$\mathrm{d}V/\mathrm{d}t$ can be calculated from the slope of V plotted against s_{xy} (see equation 5), and

$$D = m[g\sin\Theta - (\mathrm{d}V/\mathrm{d}s_{xy})V\cos\Theta]\,. \tag{8}$$

The ideal falcon

The ideal falcon in this study is an instance of the theory for ideal falcons and it serves as a standard with which we compare the real falcon. It has the same body mass (1.02 kg) and it flies in air with the density (1.05 kg m^{-3}) of the standard atmosphere (von Mises, 1959) at the temperature and altitude at which we made our observations. It has a parasite drag coefficient of 0.18, which was measured on a model body of a peregrine falcon (Tucker, 1990). There is some evidence that this value may be too high: parasite drag coefficients of manufactured objects, similar in shape to a falcon body, can be 0.07 (Tucker, 1998), and Pennycuick *et al.* (1996) have suggested a value of 0.05 for birds the size of the ideal falcon. We will show the

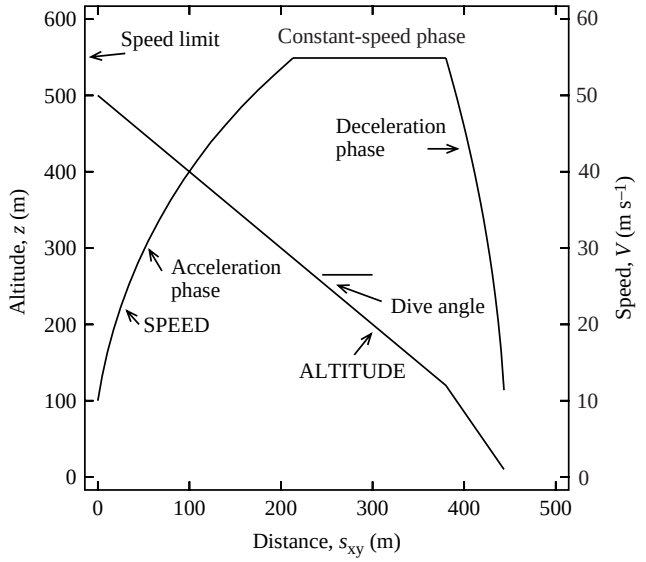

Fig. 1. Speed and altitude as functions of distance traveled over the ground in an ideal dive by an ideal falcon with a mass of 1.02 kg. The falcon minimizes its drag during the acceleration phase and increases drag at the start of the constant-speed phase. It increases drag again at the start of the deceleration phase and decelerates at −1.2 times the acceleration of gravity. The dive angle remains at 45 ° until the start of the deceleration phase, when it changes to 60 °. s_{xy}, distance along the glide path projected onto the x,y plane.

effect of a value of 0.07 on the acceleration of the ideal falcon, but otherwise use the conservative value of 0.18.

The ideal falcon performs an 'ideal dive' (Fig. 1) that resembles a typical dive observed in this study and establishes the nomenclature for different parts of the dive. The ideal dive has two straight glide paths, two dive angles and three phases. During the acceleration phase, the ideal falcon descends along a glide path with minimum drag at each speed and, consequently, accelerates at the maximum rate to a speed limit. At the speed limit, it increases its drag above the minimum and begins the constant-speed phase, during which it descends at the same glide angle but holds its speed constant. After some time at constant speed, it increases its drag again and begins the deceleration phase while more than 100 m above the ground. At this point, the dive angle increases slightly and the falcon decelerates strongly at −1.2 times the acceleration of gravity.

This controlled sequence of acceleration, constant speed, then deceleration may seem unrealistic to those who have watched falcons in long, steep dives. The birds seem to fall from the sky, steadily accelerating as they lose altitude. The falcon in this study gave the same impression, but our measurements showed that, in fact, its behavior during a dive resembled the controlled behavior of the ideal falcon.

The ideal dive has some similarities to the dives performed by human sky-divers. A sky-diver accelerates in free-fall to a speed limit of 50–60 m s^{-1} and maintains this speed by assuming a body shape that keeps drag above its minimum value (Hoerner and Borst, 1975). Eventually, the sky-diver opens a parachute and decelerates even more strongly than the falcon. For example, when a military parachute of the type used for planned jumps opens, peak deceleration may reach −3 times gravitational acceleration (calculated for a T10 parachute, Ewing *et al.* 1978).

Materials and methods

The falcon

'Kumpan', a male gyrfalcon hatched in 1992 and trained for falconry by T. J. Cade (the falconer), was the subject of these experiments. Kumpan had an unusual habit for gyrfalcons, which typically hunt by flying low over the ground (Cade, 1982): he soared in thermals to altitudes of several hundred meters above the ground and then returned to the falconer in a dive when called. We took advantage of this predictable diving behavior by using a tracking device to record Kumpan's position in three-dimensional space at 1 s intervals as he soared and at shorter intervals during his dives. We recorded 11 dives, referred to subsequently by the letters A–K.

The falconer kept Kumpan's body mass within 10 g of 1.02 kg during our observations. Kumpan was a relatively small gyrfalcon: males may have masses up to 1.5 kg and females to 2.0 kg or more. Kumpan was hungry enough at this mass to return when called and he always received food when he returned. Kumpan's total mass during flight was 22.5 g more than his body mass because he carried on his tarsi two radio transmitters and a bell that helped to locate him when he was out of sight. We assume that these items had no effect on his diving performance, because in flight he carried them tucked up under his tail where what little aerodynamic drag they might have added would tend to be compensated for by their mass.

The tracking device

The tracking device (TD, Tucker, 1995) recorded the spherical coordinates of the falcon: the distance along the line of sight (LOS) from the TD to the bird and the vertical and horizontal angles of the LOS. The operator (V. Tucker) established the LOS by following the falcon with the ×14 TD telescope, which was part of a coincidence rangefinder with a 1 m base. The operator measured the distance to the falcon by using a thumbwheel to align two images of the bird in the telescope, and transducers sent digitized information on the thumbwheel position and the two angles to a portable computer for recording.

The computer ordinarily recorded data at 1 s intervals, but it could be set to record data faster and more accurately during steep dives. The computer operator (A. Tucker) could move a switch at any time during the track to put the computer program into an irregular timing mode, in which case the computer recorded data when the vertical angle of the LOS decreased by 2.8 °, rather than every second. In this mode, the computer recorded data at rates up to twice per second.

The TD also recorded photographic data when in irregular timing mode. A 35 mm, motor-drive camera with a 500 mm

focal length mirror lens was mounted on the rangefinder and aimed along the LOS. The computer triggered the camera, waited for the shutter to open and then recorded time, range and angular data. The photographs showed the position of the falcon relative to the LOS and, if the LOS did not penetrate the falcon's image, we corrected the recorded vertical and horizontal angles to make it do so.

The protocol

We set up two stations 800 m apart, one for the falconer with Kumpan, and the other for the TD and its operators. Kumpan, hooded and with Aylmeri jesses attached to his legs (Beebe and Webster, 1964), perched on the falconer's fist. When radio communication between the stations established that everyone was ready, the falconer removed the hood and jesses, and Kumpan flew. When the three of us agreed by radio that Kumpan had reached a suitable location, ideally within 1 km of the TD and several hundred meters above the ground, the falconer called Kumpan down.

The falconer called Kumpan with a shout and by swinging a lure (Beebe and Webster, 1964) or by throwing a pheasant into the air at the beginning of a dive. The pheasant usually landed before Kumpan arrived, and Kumpan ended the dive by landing and chasing the pheasant on foot. On a few occasions, Kumpan chased the pheasant in the air for 50 m or less before the pheasant landed or was caught.

We worked with Kumpan when thermals had developed between 11:00 and 13:00 h and temperatures were near 30 °C. Kumpan usually flew for 15–30 min before he was in a good position for the falconer to call him. After the first dive, the falconer fed him and then hooded and jessed him for a 15 min rest. When everyone was again ready, the falconer released Kumpan for the second and last flight of the day.

The location and the wind

We set up the TD during August 1994 and 1995 at latitude 43° 25′ 11″ north and longitude 116° 12′ 15″ in Idaho, 16.5 km south of Boise Municipal Airport. This undeveloped location on the Snake River Plain is a sagebrush-covered flat, with a gradient of 0.006–0.01 that extends for several kilometers in all directions. It is 908 m above sea level, and the nearest regions that are 300 m or more higher are 16 km to the northeast, 42 km to the north and 46 km to the west.

We obtained the speeds and directions of winds aloft from Boise Municipal Airport, which reported values based on readings from instruments 10 m above the ground and on radiosonde measurements. Winds blew from the northern half of the compass for all but one dive. The wind speed was less than $3\,m\,s^{-1}$ for six dives, between 3 and $5\,m\,s^{-1}$ for three dives and between 6 and $7\,m\,s^{-1}$ for two dives. Since these directions and speeds were consistent with those that we observed and measured at the study site using a hand-held anemometer, and were a small fraction of the speeds that Kumpan reached in dives, we did not attempt to measure winds aloft.

Data analysis

The raw data from the computer went through several procedures before we could determine speed and dive angles from them: (1) transformation of the transducer data recorded by the computer to spherical coordinates; (2) correction of horizontal and vertical angles from photographic data; (3) range smoothing for dives C, F and I; (4) transformation to x,y,z coordinates; (5) correction for wind drift; (6) computation of V and s_{xy} with three-point moving averages; and (7) computation of dV/ds_{xy} and dz/ds_{xy} from plots of V and z against s_{xy}.

For procedure 2, we measured angular corrections from the photographs taken during the irregular timing mode and added them algebraically to the angles for the LOS calculated from the transducer data. For procedure 3, we plotted, for all dives, the range from the TD to the falcon against time. This plot showed when the TD operator moved the range thumbwheel in steps rather than smoothly while following the falcon. These steps were large enough in dives C, F and I to make the computed values for V vary excessively. We used smoothed range data for these dives, obtained from parabolic equations fitted by least squares to the stepped range data. For procedure 5, we added the wind velocity vector to the falcon's horizontal velocity vectors. For procedure 7, we found the two derivatives from the slopes of lines, fitted by least squares, to V and z for the range of s_{xy} of interest.

Error analysis

Timing errors

The time intervals (Δt) between points are accurate to within better than 0.001 s for intervals of 1 s, and to within 0.01 s for irregular intervals, when the TD was operated in the irregular timing mode. Timing errors are negligible in this study, since the falcon moved less than 0.6 m during the timing error.

Position errors

The positions of the falcon, recorded as points along the track, contain errors from two sources, aside from timing errors (Tucker, 1995): instrumental errors, due to mechanical and electronic tolerances in the TD; and operator errors, due to pointing errors and range errors. Pointing errors arise when the operator fails to keep the LOS within the outline of the falcon, and range errors arise when the operator fails to align the images of the falcon in the rangefinder. Instrumental errors are negligible compared with operator errors for a falcon in a fast, steep dive, and pointing errors are also negligible, because the TD operated in the irregular timing mode for all dives except I. In this mode, the photographs from the camera on the rangefinder allowed us to correct for pointing errors. There remain range errors, which we discuss below with data and equations from Tucker (1995).

Range errors cause errors in R, the recorded distance along the LOS to the falcon. These errors, in turn, cause errors in the falcon's computed speed, since:

$$V = R\Delta\Psi/\Delta t\,, \tag{9}$$

where $\Delta\Psi$ is the angle (in rad) between the lines of sight to successively recorded positions of the falcon, recorded at time interval Δt. We define the range error in terms of counts generated by the thumbwheel transducer, because the error expressed in counts is independent of range; i.e. a given rotation of the thumbwheel produces the same change in counts, and the same displacement of the images in the rangefinder, whatever the range (Tucker, 1995). In contrast, a range error measured in meters for a given image displacement increases as range increases. Once the range error in counts is known, it can be converted to meters at a given range (see equation 10 below).

We estimated the standard deviation of the range error during Kumpan's dives from notes made by the TD operator on his visual recollection of the misalignment of the falcon's images during a dive. These notes indicated that the operator could keep Kumpan's images in alignment within one-quarter of a body length at a range of 1000 m, 75 % of the time. We checked this estimate by tracking helium-filled balloons, 0.2 m in diameter, or approximately half Kumpan's body length. These balloons moved much more slowly than Kumpan, and the TD operator could keep their images in alignment within one-quarter of a balloon diameter essentially 100 % of the time at a range of 1000 m. A misalignment of half a diameter at this range was very obvious, and its appearance supported the TD operator's estimate that, most of the time, Kumpan's images were in better alignment.

This percentile of 75 % can be used to estimate the standard deviation (σ) of the range error, in transducer counts, assuming a normal error distribution. A misalignment of one-quarter body length corresponds to 85 transducer counts, and the estimate of σ is 85/1.15=74 counts, since 1.15σ on either side of the mean includes 75 % of the area under a normal distribution curve. We expect 95 % of our reported speeds to be within a confidence interval that extends to 2σ on either side of the true speed, independent of range.

The relationship between the range error in transducer counts (ΔC) and the fractional range error ($\Delta R/R$) is:

$$\Delta R/R = \Delta C R/(956 \times 10^3) . \quad (10)$$

The fractional range error causes a fractional speed error ($\Delta V/V$) and, from equation 9 at constant $\Delta\Psi/\Delta t$:

$$\Delta V/V = \Delta R/R . \quad (11)$$

For example, when ΔC=2σ and R=1000 m (a typical value for this study; see Table 1), then, from equations 10 and 11, $\Delta V/V$=0.16 for σ=74. Hence, we expect the reported speeds in a dive at this range to be within 16 % of the true speed, 95 % of the time.

Results

Pre-dive behavior

When the falconer removed Kumpan's hood and jesses, Kumpan took off and flew low over the ground for a minute or two before climbing by soaring in a thermal, but from then on, his behavior was less predictable. If things went well, he remained within 1.5 km of the TD, and we tracked him from the falconer's fist to a position where he was circling within 1 km of the TD and approximately 500 m above the ground. The falconer then called Kumpan, who immediately stopped circling and dived directly to the falconer, gradually folding up his wings as he picked up speed. When he landed, the falconer picked him up, fed him and hooded him.

However, not all of Kumpan's flights fitted this pattern. He often flew more than 3 km from the TD, and we lost sight of him in haze or clouds. Usually he returned within approximately 30 min to a location where the falconer could find him by searching the sky with binoculars in a direction indicated by a radio receiver tuned to one of the transmitters that Kumpan carried. Usually the TD operators could not see Kumpan in such circumstances and were unable to track him when he dived.

Sometimes the situation was reversed, and the operators at the TD could see Kumpan when the falconer could not. The computer operator then used the radio to report Kumpan's location and to ask the falconer to call the unseen bird. The falconer watched in the expected direction after calling, and Kumpan usually appeared in a few seconds, approaching rapidly. We recorded some good dives using this method.

Besides disappearing, Kumpan had several other nervewracking behaviors – chasing other birds and even a nearby train, and fighting with hawks and eagles in the vicinity – but he always returned unscathed.

Dive altitudes, angles and speeds

We tracked Kumpan during 11 dives (summarized in Fig. 2

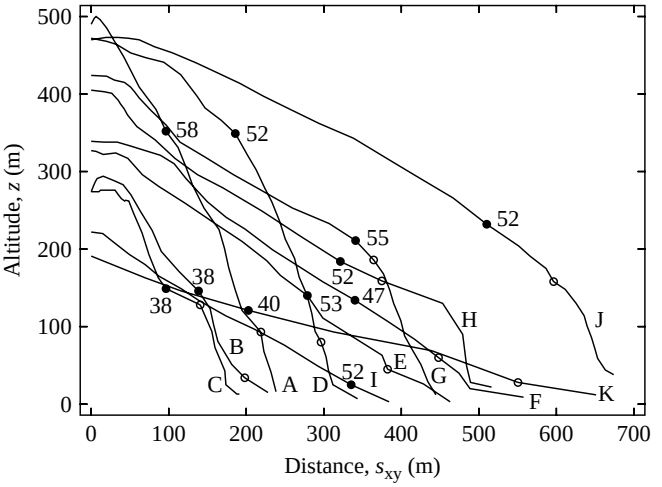

Fig. 2. Altitudes as functions of distance traveled over the ground in 11 dives by a 1.02 kg gyrfalcon. The letters identify the dives, from steepest (A) to shallowest (K). The filled circles mark the ends of the acceleration phases, and the numbers adjacent to them show the speeds (in m s^{-1}) at these points. The open circles mark the starts of the deceleration phases. s_{xy}, distance along the glide path projected onto the x,y plane.

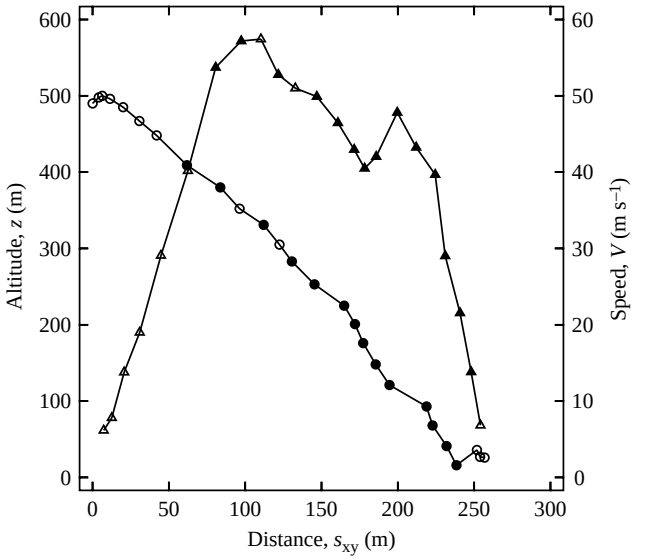

Fig. 3. Speed (triangles) and altitude (circles) during a steep dive (dive A at 62 °) by a 1.02 kg gyrfalcon. The open symbols are data recorded at 1 s intervals, and the filled circles are data recorded at irregular intervals and accompanied by photographs (see Materials and methods). s_{xy}, distance along the glide path projected onto the *x*,*y* plane.

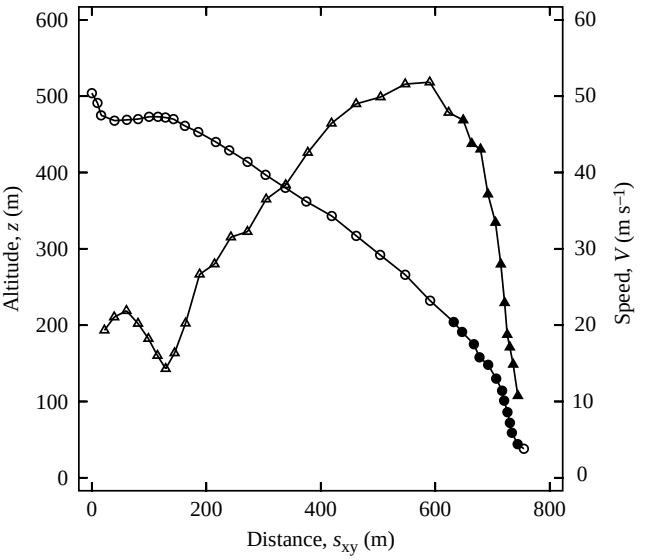

Fig. 4. Speed (triangles) and altitude (circles) during a shallow dive (dive J at 26 °) by a 1.02 kg gyrfalcon. The open symbols are data recorded at 1 s intervals, and the filled circles are data recorded at irregular intervals and accompanied by photographs (see Materials and methods). s_{xy}, distance along the glide path projected onto the *x*,*y* plane.

and Table 1) that started at altitudes 200–500 m above the ground and had dive angles of 17–62 ° during the acceleration phases of the dives. In most dives, Kumpan accelerated to speed limits between 52 and 58 m s^{-1} before beginning the constant-speed phase of the dive and maintained these speeds without change in dive angle until his altitude decreased to 185 m or less above the ground. Then he entered the deceleration phase of the dive and often increased his dive angle (see dives A, D, G, H and J). (In dive I, we could not follow Kumpan to his speed limit, because he dropped below the skyline, and was not visible against the distant mountains.)

Example dives

Figs 3 and 4 show altitudes and speeds for a steep and a shallow dive (dives A and J), plotted against s_{xy}, the distance traveled on the *x*,*y* plane. These dives were typical, and the characteristics of dives at other angles may be inferred from them.

Table 1. *Characteristics of 11 dives by a gyrfalcon* Falco rusticolus

Dive	Range	Θ_1	Θ_2	V_1	V_2	V_3	$\bar{D}_1$	$\bar{D}_2$	Deceleration (***g***)
A	1007	62	69	58	40	7	0.36	2.66	–1.55
B	800	56	37	38	38	12	0.21	2.06	–0.64
C	935	56	56	38	30	10	0.21	2.51	–1.25
D	754	42	73	52	50	25	0.43	2.02	–0.97
E	866	38	38	53	50	29	0.48	3.17	–1.33
F	811	34	34	47	45	35	0.47	2.39	–0.77
G	766	32	66	55	50	21	0.60	1.88	–0.81
H	1170	32	69	52	40	30	0.55	1.70	–0.65
I	1266	30	–	52	–	52	0.58	–	–
J	595	26	60	52	43	11	0.67	2.33	–1.14
K	897	17	17	42	40	38	0.78	2.21	–0.36

Range, distance (m) from tracking device to falcon at the start of the dive; Θ_1, dive angle (degrees) at end of acceleration phase; Θ_2, dive angle (degrees) at start of deceleration phase; V_1, speed (m s^{-1}) at end of acceleration phase; V_2, speed (m s^{-1}) at start of deceleration phase; V_3, speed (m s^{-1}) at end of track; $\bar{D}_1$, $D/(mg\sin\Theta)$ at V_1 in acceleration phase; $\bar{D}_2$, $D/(mg\sin\Theta)$ at V_2 in deceleration phase; $\bar{D}$ is dimensionless drag, where D is aerodynamic drag, m is mass and g is the the magnitude of gravitational acceleration.

Deceleration (measured as a multiple of g) is given at V_2 in deceleration phase.

In dive I, Kumpan dropped below the skyline, so values from the deceleration phase could not be measured.

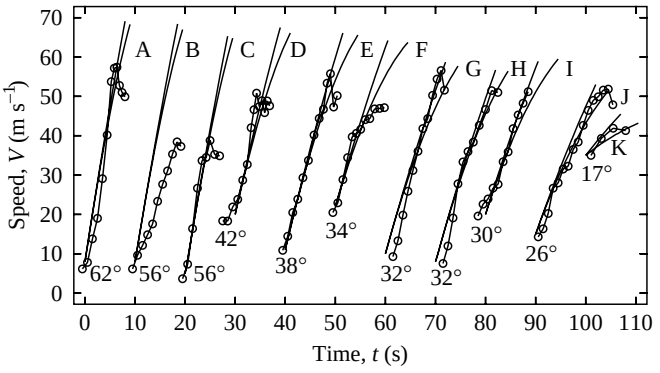

Fig. 5. Speed as a function of time in 11 dives by a 1.02 kg gyrfalcon. The letters identify the dives, and the numbers show dive angles, from steepest (A) to shallowest (K). Open circles show measured data for the gyrfalcon; the adjacent pair of smooth curves brackets the speeds of the ideal falcon at the same dive angle, but with different parasite drag coeffcients: 0.07 for the steeper curve and 0.18 for the other curve (see text for additional explanation). The smooth curves continue beyond the measured data at the ends of the acceleration phase.

Acceleration, dive angles and speed limits during the acceleration phase

Kumpan accelerated more rapidly the steeper the dive angle, as can be seen from the slopes of the curves for speed plotted against time (Fig. 5), which also shows two curves for the ideal falcon diving at each indicated dive angle with minimum drag but different parasite drag coefficients: 0.07 for the steeper curve and 0.18 for the other (see Theory section). Both curves use the same relationship between lift coefficient and profile drag coefficient. Kumpan clearly stopped accelerating at speed limits well below the terminal speeds for each dive angle, since the ideal falcon is still accelerating rapidly at the real falcon's speed limits.

Kumpan's performance and that of the ideal falcon are quite similar during the acceleration phase: in each dive, Kumpan had an essentially constant dive angle, progressively folded his wings as he picked up speed and usually accelerated at approximately the same rate as the ideal falcon at the same dive angle. Whether the parasite drag coefficient is 0.07 or 0.18 makes little difference at speeds less than 40 m s^{-1}. These similarities suggest that, in most dives, Kumpan arranged himself to have minimum drag during the acceleration phase, but abruptly increased his drag by a factor of 1.3 to 4.8 at a speed limit.

The steeper curves for the ideal falcon with a parasite drag coefficient of 0.07 fit the data better for all dives except B, suggesting that this coefficient may indeed be less than 0.18, as mentioned in the Theory section. However, a quantitative estimate of the parasite drag coefficient from the diving data requires a theoretical analysis that is beyond the scope of the present study.

The amounts by which drag increases at the speed limits can be estimated since drag during the constant-speed phase is $mg\sin\Theta$. The drag just before acceleration ceases, estimated from that of the ideal falcon, is 20–80 % of the drag in the constant-speed phase, depending on the glide angle (Table 1).

Constant-speed phase

Kumpan's speed in the constant-speed phase was constant in a relative sense: it changed more slowly than in the acceleration and deceleration phases. Fig. 2 shows the altitudes at which Kumpan began and terminated the constant-speed phases of his dives. In dives C, G, H and J, the duration of the constant-speed phase was near zero, and in others it lasted a few seconds. The example dives (Figs 3, 4) illustrate these two extremes.

Kumpan ended the constant-speed phase by increasing his drag again and decelerating strongly; his drag after this increase can be estimated from his dive angle and deceleration (equation 7). Drag at the end of the constant-speed phase increased to 1.7–3.2 times the drag during this phase (Table 1).

Deceleration phase

All dives (except I) included a deceleration phase; and in 8 of these 10 dives, the dive angle remained the same or increased during deceleration. The magnitude of deceleration, expressed as a multiple of gravitational acceleration, varied widely, with a mean value of $-0.95\,g$ (Table 1).

Discussion

The speeds of 47–58 m s^{-1} reported for 8 of the 11 dives in this study are the highest ever measured for animals with methods of known accuracy. The previous record was 43 m s^{-1} for a flock of mergansers (*Mergus serrator*) (Alerstam, 1987). Even so, Kumpan could have gone faster if he had not controlled his speed by increasing drag. For example, the ideal falcon with minimum drag can reach a speed of 72 m s^{-1} in a 45 ° dive with a vertical drop of 450 m, starting from 15 m s^{-1}, and speeds of 100 m s^{-1} or more are plausible in steeper dives with vertical drops of over 1000 m (Tucker, 1998). Kumpan's dives, however, were controlled maneuvers in which he increased drag in two large and distinct steps: first, to maintain a speed limit after acceleration, and a second time to begin decelerating from the speed limit.

We controlled several of the conditions under which Kumpan made his dives and, in other circumstances, he might have chosen to fly faster. First, we shall discuss how he might have increased his drag in a dive, and then we shall discuss how the circumstances of a dive might influence the decision of a falcon to limit its speed; i.e. its strategy in a dive.

Control of drag by shape changes

Kumpan increased his drag at the ends of the acceleration and constant-speed phases by changing his body shape. Some changes would have been obvious through the TD telescope while others would not. Obvious changes included spreading his wings widely or lowering his tarsi and feet from their normal position tucked under the tail. Falcons and other birds often take these actions before landing and accompany them

with an upward pitch of the body by 30 ° or more and by spreading the tail. Falcons may also take them just before striking prey, and Kumpan took them at the end of the deceleration phase as he approached the falconer. However, we did not see these or any other changes through the TD telescope as Kumpan changed from the acceleration phase to the constant-speed phase and, finally, to the deceleration phase.

Changes that would not have been obvious include smaller pitching or yawing movements of the body and small increases in wing span and wing angle of attack. Yawing (which is frequent in dives) and pitching increase the body (parasite) drag, and the wing changes may increase the wing drag. However, increases in wing span and angle of attack can also increase lift, and a falcon on a straight glide path has constant lift. Otherwise, the falcon would pull out of the dive, and Kumpan did not pull out of his dives until the end of the deceleration phase.

Falcons hold their wings in a cupped position while diving and may be able to increase the drag of the wings without increasing lift (Tucker, 1998). The wings are cupped around the body, as in perching, but with spaces between their undersides and the body. Increasing the angle of attack of cupped wings increases the aerodynamic forces that they produce, but these forces have lateral components that cancel one another. The result can be an increase in drag but not lift.

The ideal falcon can generate enough drag with cupped wings both to stop accelerating in a dive and to decelerate at $-1.5\,g$. The amount of drag that a real falcon can generate with cupped wings has not been measured but, if Kumpan's aerodynamics are like those of the ideal falcon, he could have increased his drag to the values shown in Table 1 by increasing the angle of attack of his cupped wings by an amount that would have been unnoticeable through the TD telescope.

In fact, the falconer was close to Kumpan at the end of a dive and could see that he did appear to increase the angle of attack of his cupped wings during the deceleration phase. He held the leading edges of his wings away from his body, but held his wing tips against his tail and confluent with it. In this position, a line between the wrist on the leading edge and the wing tip made an angle of 10–15 ° with the glide path, and a conventional wing with an angle of attack this high would be approaching stall and have high drag.

Strategy

Kumpan had to make several decisions to execute a dive, and these decisions presumably depended on the conditions under which he made the dive. A wild falcon may experience very different conditions and, in this section, we discuss how a wild falcon's diving behavior might differ from that of Kumpan.

We controlled four conditions that seem particularly relevant to Kumpan's diving behavior: (1) the falconer called for a dive by presenting a lure or a pheasant near the ground; (2) Kumpan had to be flying in a certain region of space near the TD before the falconer called for a dive; (3) the falconer was on the ground and occupied the same position from which Kumpan flew from the falconer's fist; (4) Kumpan always received food when he landed in the vicinity of the falconer.

Given these conditions, Kumpan's strategy was to await the call while gliding, usually within 2000 m of the falconer and at an altitude of 200 m or more above the ground. He began most dives by approaching the falconer as fast as he could up to a speed limit, reached while he was still more than 100 m above the ground (Fig. 2). He began to slow down when still 50 m or more above the ground, and he approached the ground with a nearly unchanged dive angle.

He could have arrived at much higher speeds, and still not crashed into the ground, by dispensing with the constant-speed and deceleration phases, and accelerating with an unchanged dive angle until near the ground. He could then have pulled out of the dive with a small additional loss of altitude. For example, we noted above that the ideal falcon could reach a speed of $72\,m\,s^{-1}$ with a 450 m drop in a 45 ° dive. It could pull out of this dive with an additional vertical drop of 14 m (Tucker, 1998).

Falcons presumably approach prey at a speed that balances the risk of injuring themselves against the risk of failing to catch prey and, given the conditions for Kumpan's dives, the balance of risks should favor low speeds. The lure or pheasant was on or near the ground, and a low-speed approach would decrease the risk of crashing into the ground. A low-speed approach to the lure would not increase the risk of failure because Kumpan was always fed at the end of the action. Nor would the risk increase much when diving at the pheasant, since Kumpan usually had to land to make the catch.

Wild falcons dive under different conditions that in many cases would favor high-speed approaches. In fact, we have preliminary measurements of speeds in excess of $70\,m\,s^{-1}$ in wild peregrines (*Falco peregrinus*, a species with a mean weight approximately half that of gyrfalcons). Peregrines prey almost exclusively on birds seized or struck in the air, often at the end of a long, steep dive, and they often beat their wings to build up speed before entering a dive. Since the prey may be high in the air, the risk of a crashing into the ground at the end of a dive is low, and high speed allows a fast, perhaps unobserved, approach and a better chance of overtaking a fleeing prey and striking it hard.

However, high speeds could have disadvantages. A falcon at high speed risks injuring itself when striking prey and has reduced maneuverability although a peregrine that fails to strike the prey on the first approach may use its speed to pull out of the dive, loop back and strike again, often several times. Peregrines appear to turn in remarkably short distances, and the model for ideal falcons provides an explanation for this ability: ideal falcons, like real falcons, flex their wings, and flexed wings at high speeds can generate forces that cause accelerations more than 10 times the acceleration of gravity (Tucker, 1998). As a result, body parts such as the head may have apparent weights of more than 10 times those in constant-speed flight. The compact, robust bodies of falcons seem to be well-suited for tolerating these forces.

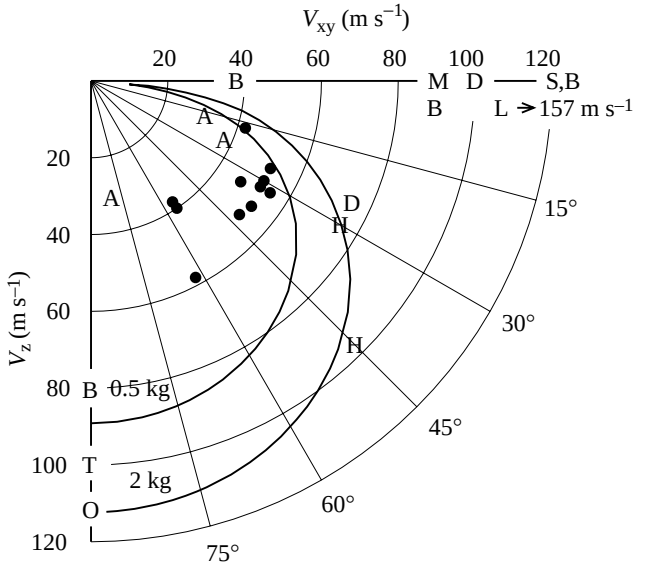

Fig. 6. A velocity polar diagram for several estimated and measured velocities of diving falcons. The axes show the horizontal component (V_{xy}) and the vertical component (V_z, plotted downwards) of the diving velocities; the rays (light lines) show dive angles at 15 ° intervals and the light circular arcs show diving speeds at 20 m s^{-1} intervals, as indicated on the horizontal and vertical axes. The bold curves (from Tucker, 1998) show the terminal speeds of ideal falcons, with masses of 0.5 and 2 kg and minimum drag, diving at various angles at sea level (air density 1.23 kg m^{-3}). The filled circles (slightly displaced in cases of overlap) show the dive angles and speed limits for the 11 dives in this study. The capital letters indicate authors of other studies (see letter code below) and are centered over values from these studies, except for L, which indicates an off-scale speed of 157 m s^{-1}. Letters on or near the V_{xy} axis show speed estimates for which no dive angles were given. A, Alerstam (1987); B, Brown (1976); D, Dement'ev (1951); H, Hangte (1968); L, Lawson (1930); M, Mebs (1975); O, Orton (1975); S, Savage (1992); T, Tucker and Parrott (1970).

High speeds expose falcons to large accelerations even during straight flight. For example, Kumpan's mean deceleration during the deceleration phases of his dives exceeded that of an automobile during maximum braking. Decelerations during braking are limited to less than a typical value of $-0.8\,g$ by the coefficient of friction of the tires on a dry road (Limpert, 1992).

There may be disadvantages to high speed that we have not mentioned. For example, aerodynamic instability may develop, and large aerodynamic forces might arise that could interfere with vision and breathing or even strip the falcon of feathers. Collisions with insects could also be dangerous.

Comparison with wild falcons

Many authors have estimated the speeds of wild falcons in dives (Fig. 6), but only Alerstam (1987) and the present study have measured diving speeds with methods of known accuracy. Alerstam (1987) used radar to track a wild peregrine *Falco peregrinus* during three dives that started 374–1022 m above the ground, with dive angles of 25–64 °. This bird held its speeds to 39 m s^{-1} or less, averaged over 10 s intervals, and Clark (1995) questions whether peregrines exceed 41 m s^{-1} in dives. Kumpan exceeded 41 m s^{-1} and could have gone faster, and Alerstam's peregrine might have exceeded this speed if it had controlled its speed by alternately accelerating and decelerating. In this case, higher speeds could have been hidden by the 10 s averaging interval for the radar measurements, compared with the 1 s intervals used in the present study. It will be interesting to measure the diving behavior of other falcons to see whether they too limit their speeds and at what levels.

List of symbols

C	range transducer counts
D	aerodynamic drag
$\bar{D}$	dimensionless drag
g	magnitude of gravitational acceleration
m	body mass
R	distance from tracking device to falcon
s	distance along the glide path
s_{xy}	distance along the glide path projected onto the x,y plane
t	time
V	speed along glide path
V_e	speed limit
V_E	terminal speed
V_{xy}	horizontal velocity component
V_z	vertical velocity component
x, y, z	spatial coordinates
Θ	dive angle
σ	standard deviation of range transducer counts
Ψ	angle of the line of sight to the falcon

This study was partially supported by a grant (DEB-9107222) from the National Science Foundation and a grant dated 25 April 1995 from the Duke University Arts and Sciences Research Council. We are grateful to The Peregrine Fund of Boise, Idaho, for providing laboratory space.

References

ALERSTAM, T. (1987). Radar observations of the stoops of the peregrine falcon *Falco peregrinus* and the goshawk *Accipiter gentilis*. *Ibis* **129**, 267–273.

BEEBE, F. L. AND WEBSTER, H. M. (1964). *North American Falconry and Hunting Hawks*. Denver: North American Falconry and Hunting Hawks.

BROWN, L. A. (1976). *British Birds of Prey*. London: Collins.

CADE, T. (1982). *The Falcons of the World*. Ithaca: Cornell University Press.

CLARK, W. S. (1995). How fast is the fastest bird? *WildBird* **9**, 42–43.

DEMENT'EV, G. P. (1951). Order Falconiformes (Accipitres). Diurnal raptors. In *Birds of the Soviet Union*, vol. 1 (ed. G. P. Dement'ev and N. A. Gladkov), pp. 71–379. Jerusalem: Israel Program for Scientific Translation, 1966.

EWING, E. G., BIXBY, H. W. AND KNACKE, T. W. (1978). *Recovery System Design Guide*. Technical Report AFFDL-TR-78–151, Wright-Patterson Air Force Base, Ohio: Air Force Flight Dynamics Laboratory, AF Wright Aeronautical Laboratories, AFSC.

HANTGE, T. (1968). Zum Beuteerwerb unserer Wanderfalken (*Falco peregrinus*). *Orn. Mitt.* **20**, 211–217.

HOERNER, S. F. AND BORST, H. V. (1975). *Fluid Dynamic Lift*. Bricktown, NJ: L. A. Hoerner.

LAWSON, R. (1930). The stoop of a hawk. *Essex Co. Orn. Club* pp. 79–80.

LIMPERT, R. (1992). *Brake Design and Safety*. Warrendale: Society of Automotive Engineering.

MEBS, T. (1975). Falcons and their relatives. In *Grzimek's Animal Life Encyclopedia*, vol. 7 (ed. B. Grzimek), pp. 411–431. New York: Von Nostrand Reinhold Co.

ORTON, D. A. (1975). The speed of a peregrine's dive. *The Field* (September), 588–590.

PENNYCUICK, C. J., KLAASSEN, M., ANDERS, K. AND LINDSTRÖM, A. (1996). Wingbeat frequency and the body drag anomaly: wind-tunnel observations on a thrush nightingale (*Luscinia luscinia*) and a teal (*Anas crecca*). *J. exp. Biol.* **199**, 2757–2765.

SAVAGE, C. (1992). *Peregrine Falcons*. San Francisco: Sierra Club.

TUCKER, V. A. (1990). Body drag, feather drag and interference drag of the mounting strut in a peregrine falcon, *Falco peregrinus*. *J. exp. Biol.* **149**, 449–468.

TUCKER, V. A. (1995). An optical tracking device for recording the three-dimensional paths of flying birds. *Rev. Sci. Instrum.* **66**, 3042–3047.

TUCKER, V. A. (1998). Gliding flight: speed and acceleration of falcons during diving and pull out. *J. exp. Biol.* **201**, 403–414.

TUCKER, V. A. AND PARROTT, G. C. (1970). Aerodynamics of gliding flight in a falcon and other birds. *J. exp. Biol.* **52**, 345–367.

VON MISES, R. (1959). *Theory of Flight*. New York: Dover Publications.